

Uniform carbon-covered titania and its photocatalytic property

L. Lin^a, W. Lin^a, Y.X. Zhu^{a,*}, B.Y. Zhao^a, Y.C. Xie^a, Y. He^b, Y.F. Zhu^b

^a State Key Laboratory for Structural Chemistry of Unstable and Stable Species, College of Chemistry and Molecular Engineering, Peking University, 100871 Beijing, China

^b Department of Chemistry, Tsinghua University, 100084 Beijing, China

Received 22 February 2005; received in revised form 12 April 2005; accepted 12 April 2005

Available online 23 May 2005

Abstract

A series of carbon-covered titania (CCT) were prepared via pyrolysis of sucrose highly dispersed on the surface of titania in flowing N₂. The samples were characterized by XRD, BET, DTA–TG, UV–vis, and their photocatalytic properties were evaluated with a model pollutant, methylene blue (MB), at room temperature. It is found that carbon coverage inhibits the phase transformation of TiO₂ and makes the absorption edge of titania shift to the visible region. Photocatalytic tests show that under UV illumination, the kinetics of the dyes' elimination in the suspension of CCT powders follows an apparent first-order rate as in pure titania suspension, but the rate constant is much higher than that of pure titania, even commercial Degussa P-25 TiO₂. In addition, as a photocatalyst responsive to visible light, CCT shows similar kinetic features for the photodegradation of the dyes under visible light illumination to that under UV illumination. From the detection of the products of MB degradation, and the absorption spectra of MB solution after the photocatalytic reaction, it is proved that MB is decomposed over CCT samples under visible light illumination, whereas it is simply bleached over pure titania at the same condition.

© 2005 Elsevier B.V. All rights reserved.

Keywords: Carbon-covered titania; Carbon; Sucrose; Photocatalysis; Methylene blue

1. Introduction

The photocatalytic decomposition of pollutants in water and air has attracted much interest for decades [1]. Among various semiconduct materials (oxides, sulfides, etc.) most attention has been given to TiO₂ because of its high photocatalytic activity, resistance to photocorrosion, photostability, low cost and non-toxicity. However, titania has a large band gap (3.20 eV for anatase TiO₂) and therefore only the small UV fraction of solar light, about 2–3%, can be utilized. Many attempts have been made to sensitize titanium dioxide for the much larger visible fraction, such as transition metal deposition [2–4] or anionic species (C, N, F, S, or P) doping [5–19].

Among various modified titania, carbon–titania composites [20–29] have been reported as a kind of promising photocatalyst. Hermann and co-workers [20–22] investigated the influence of different activated carbons on the

photocatalytic degradation of aqueous organic pollutants by UV-illuminated titania (Degussa P-25). They proved that the addition of activated carbon to titania slurry under UV illumination can induce a beneficial effect on the photocatalytic degradation of phenol, 4-chlorophenol and herbicide in dependence on the properties of activated carbon. But non-addition adsorption capacities were observed. Inagaki and co-workers [23–24] found that under UV illumination TiO₂-mounted exfoliated graphite and TiO₂-mounted activated carbon could also efficiently adsorb and photodegrade heavy oil and phenol, respectively. They also proved that carbon-coated anatase-type TiO₂ could keep almost the same photocatalytic activity as that without the carbon coating [25–28]. What is more, the carbon coating could suppress the phase transformation of titania at high temperature. Kisch and co-workers [7,14] proved that carbon-containing titania, which was prepared by a modified sol–gel process using different alkoxide precursors, was able to photodegrade *p*-chlorophenol (4CP) with visible light ($\lambda > 400$ nm). It was shown that pyrolysis of alcohols employed in the

* Corresponding author. Tel.: +86 10 62751703; fax: +86 10 62751725.
E-mail address: zhuyx@pku.edu.cn (Y.X. Zhu).

sol–gel process led to carbonaceous species embedded in the TiO₂ matrix, which were responsible for the observed photosensitization. But it is hard to control the content of carbon in the carbon-containing titania as-prepared. Besides this preparation method, carbon-doped titania can also be prepared by oxidation of a titanium metal sheet in a natural gas flame [5] or oxidative annealing of TiC [8].

Recently, a simple process has been developed by our group for the preparation of uniform carbon-covered alumina (CCA) via pyrolysis of sucrose highly dispersed on the surface of alumina [30]. It is proved that this preparation method has good reproducibility, and carbon covers the surface of alumina uniformly in the as-prepared samples. In addition, the coverage and number of carbon layers in CCA can be easily controlled by changing the sucrose content in the precursors and the impregnation times. In the present work, carbon-covered titania (CCT) was prepared in the same way, and it is proved that this material shows unique adsorptive and photocatalytic properties. For organic reactant, methylene blue (MB), CCT shows much higher photoactivity than pure titania under UV illumination. And it is worthy to note that carbon coverage makes the absorption edge of titania shift to the visible region and therefore MB can be decomposed over CCT samples under visible light illumination, whereas it is simply bleached over pure titania at the same condition.

2. Experimental

2.1. Catalyst preparation

2.1.1. Preparation of TiO₂

TiO₂ was prepared by dropping aqueous solution of Ti(SO₄)₂ and 3 mol L⁻¹ NH₃·H₂O simultaneously into a beaker containing a small amount of 0.5 mol L⁻¹ NH₄HCO₃ solution with subsequent filtering and washing until no SO₄²⁻ could be detected by 0.5 mol L⁻¹ barium nitrate solution in the filtrate. The product was dried at 90 °C and then calcined in a muffle furnace at 450 °C for 4 h.

2.1.2. Preparation of catalysts

Sucrose/TiO₂ precursors were prepared by impregnating titania with aqueous solutions of sucrose. After drying at 90 °C, the precursors were calcined at 400, 500 or 600 °C in flowing N₂ with a rate of 50 mL min⁻¹ for 2 h. The preparation conditions and loadings of sucrose in the precursors

are listed in Table 1. Similarly, pure titania was treated at the same temperature as reference samples. Sucrose carbon was prepared via pyrolysis of sucrose at 500 °C in flowing N₂ for 2 h as mentioned above.

2.2. Photocatalytic decomposition of methylene blue

Photocatalytic experiments in the aqueous phase were carried out with catalyst powder suspended in a water-cooled cylindrical 250 mL Pyrex glass vessel; the suspension was stirred magnetically in the darkness or under visible light or UV illumination. The visible light source was a 150 W halogen–tungsten lamp (Phillips) equipped with a UV cut-off filter to remove the UV portion of the illumination (<420 nm). UV illumination was provided by an 8 W medium-pressure mercury lamp with a main emission peak at 365 nm (Institute of Electrical Light Source, Beijing, China).

Methylene blue (C₁₆H₁₈N₃S) was dissolved in distilled water to concentration of 1.2 × 10⁻⁵ mol L⁻¹. Powder sample of 25.0 mg was dispersed into 200 mL MB solution. Variations in the concentration of dyes were monitored by UV–vis spectroscopy at the wavelength of 665 nm after 2 h magnetically stirring in darkness to secure the adsorption–desorption equilibrium. Four millilitres of suspension was taken out at a given time intervals and immediately centrifuged at 80 rpm for 15 min, and then filtered through a 0.2 μm membrane filter to remove the particles before subjecting to UV–vis spectroscopy. The product of MB degradation was determined by ion chromatograph with a conductivity detector (ICS2500, Dionex).

Long-time stability tests were carried out in the same way as adopted by Lettmann et al. [14]. A 10-fold amount of sample was suspended in 200 mL 1.2 × 10⁻⁴ mol L⁻¹ MB solution (10-fold concentration compared to the standard activity tests as above-mentioned). This suspension was irradiated for a total reaction time of 192 h. After 96 h with 24 h increments, 20 mL of suspension was taken out and then separated by centrifuge, viz., aliquots of 25 mg of the used catalyst have been separated and subjected to standard reaction conditions for activity determination as above-mentioned.

2.3. Characterization techniques

2.3.1. BET surface area

Specific surface area was determined by using BET method based on N₂ adsorption at 77 K with a Micromeritics

Table 1
Precursor composition, carbon content and BET surface area of samples

Sample	Weight ratio of sucrose to titania in precursor	CT ^a (°C)	Carbon content (wt.%)	BET surface area (m ² g ⁻¹)
TiO ₂ -400	0	400	0	105
TiO ₂ -500	0	500	0	100
TiO ₂ -600	0	600	0	98
CCT008-400	0.08:1	400	2.1	103
CCT008-500	0.08:1	500	1.8	98
CCT008-600	0.08:1	600	1.6	96

^a Calcination temperature.

ASAP 2010 Analyzer. The samples were degassed in vacuum (10^{-3} Pa) for 2 h at 300°C prior to adsorption measurements.

2.3.2. X-ray powder diffraction

Phase composition of the samples was determined with a Rigaku D/MAX-200 X-ray powder diffractometer with Ni-filtered $\text{Cu K}\alpha$ radiation at 40 kV and 100 mA. The amount of residual crystalline sucrose can be determined by XRD quantitative phase analysis. $\alpha\text{-Al}_2\text{O}_3$ as an inner standard was added to sucrose/ TiO_2 samples, and measure the peak area for reflections 1 1 1 and 2 1 0 of sucrose and 1 1 3 of $\alpha\text{-Al}_2\text{O}_3$. The peak intensity ratio $I_{\text{sucrose}}/I_{\alpha\text{-Al}_2\text{O}_3}$ is reasonably assumed to be proportional to the ratio of the content of crystalline sucrose to that of $\alpha\text{-Al}_2\text{O}_3$, as

$$\frac{I_{\text{sucrose}}}{I_{\alpha\text{-Al}_2\text{O}_3}} = \frac{k \times X_{\text{sucrose}}}{X_{\alpha\text{-Al}_2\text{O}_3}}$$

where I and X stand for XRD intensity and weight percentage, respectively, and k is a proportionality constant determined from a sample of known phase composition. With known content of $\alpha\text{-Al}_2\text{O}_3$, the weight percentage of crystalline sucrose can be derived from the intensity ratio of $I_{\text{sucrose}}/I_{\alpha\text{-Al}_2\text{O}_3}$.

2.3.3. DTA–TG

Carbon content in the sample was determined by DTA–TG test performed on a Dupont model 1090 apparatus from room temperature to 600°C at a constant rate of $10^{\circ}\text{C min}^{-1}$ under air with a flow rate of 50 mL min^{-1} , using $\alpha\text{-Al}_2\text{O}_3$ as reference.

2.3.4. UV–vis diffuse reflectance spectra

The UV–vis spectra of the powder samples were recorded on a Shimadzu UV 3100 PC, UV–vis–NIR scanning spectrophotometer equipped with a diffuse reflectance accessory.

3. Results and discussion

3.1. Structure and morphology of carbon-covered TiO_2

Fig. 1A shows the X-ray diffraction patterns of sucrose/ TiO_2 precursors with different sucrose loadings. It can be seen that the precursors with low sucrose loading show no peaks of crystalline sucrose, while the precursors with higher sucrose loading ($>0.50 \text{ g sucrose g}^{-1}$ titania) exhibit peaks characteristic of crystalline sucrose and the intensity of these peaks increases with the increasing sucrose loading. The results of XRD analysis indicate that sucrose is highly dispersed on the surface of titania when the sucrose loading is low, while crystalline sucrose appears when the sucrose loading exceeds a certain value. The amounts of residual crystalline sucrose in the samples can be determined by XRD quantitative phase analysis [31–32]. Fig. 1B shows the residual crystalline sucrose as a function of sucrose loading. A threshold at about $0.41 \text{ g sucrose g}^{-1}$ titania corresponding to the dispersion capacity of sucrose on TiO_2 can be obtained.

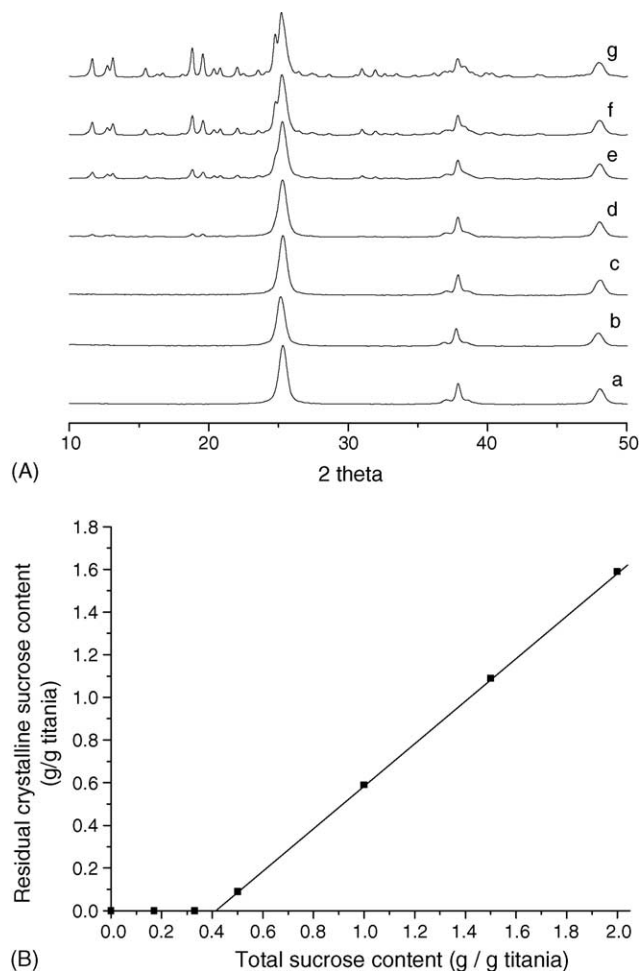


Fig. 1. (A) The XRD patterns of: (a) TiO_2 ; (b) $0.10 \text{ g sucrose g}^{-1} \text{TiO}_2$; (c) $0.33 \text{ g sucrose g}^{-1} \text{TiO}_2$; (d) $0.50 \text{ g sucrose g}^{-1} \text{TiO}_2$; (e) $1.00 \text{ g sucrose g}^{-1} \text{TiO}_2$; (f) $1.50 \text{ g sucrose g}^{-1} \text{TiO}_2$; (g) $2.00 \text{ g sucrose g}^{-1} \text{TiO}_2$. (B) Content of residual crystalline sucrose vs. total content of sucrose in samples.

It is reasonable to speculate that the morphology of carbon pyrolyzed from sucrose highly dispersed on the surface of titania will be different from carbon pyrolyzed from crystalline sucrose. As shown in Fig. 2, CCT04 prepared via pyrolysis of $0.40 \text{ g sucrose g}^{-1}$ titania in which sucrose is highly dispersed on the surface of titania, has similar pore size distribution as that of pure titania. In contrast, CCT05 prepared via pyrolysis of $0.50 \text{ g sucrose g}^{-1}$ titania, in which the residual crystalline sucrose exists, has a new peak at pore diameter of 2–4 nm in its pore size distribution. As analyzed above, these small pores can be attributed to separate carbon aggregate formed by pyrolysis of the surplus crystalline sucrose. These results are similar to what we observed in carbon-covered-alumina samples [31]. Therefore, CCT samples resulted from precursors with low sucrose loading should have uniform carbon deposition. In addition, the similar surface areas of CCT008 and corresponding pure titania as shown in Table 1 also supports this point [33].

XRD phase analysis proves that carbon covering on the surface of titania can improve the thermal stability of titania.

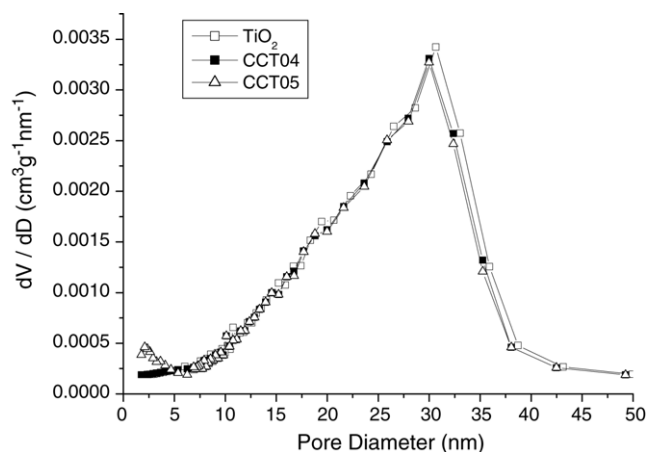


Fig. 2. Pore size distributions for TiO₂, CCT04 and CCT05.

The XRD patterns of CCT04-600 and CCT04-700 resulted from the pyrolysis of 0.40 g sucrose g⁻¹ titania at 600 and 700 °C, respectively, are compared with corresponding pure titania (labeled as TiO₂-600 and TiO₂-700) in Fig. 3. The pure

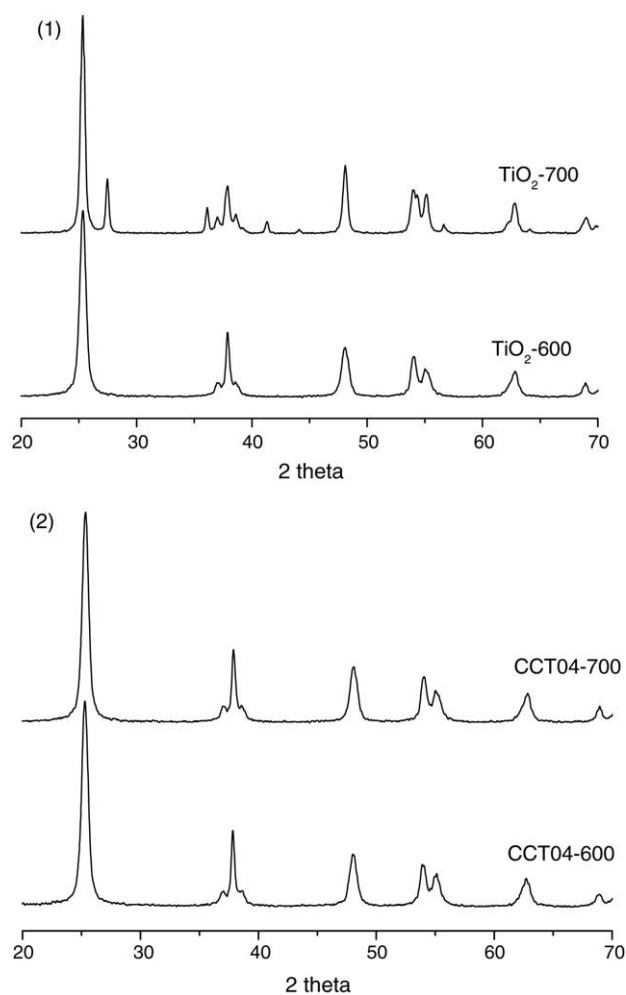


Fig. 3. The XRD patterns of (1) TiO₂-600 and TiO₂-700; (2) CCT04-600 and CCT04-700.

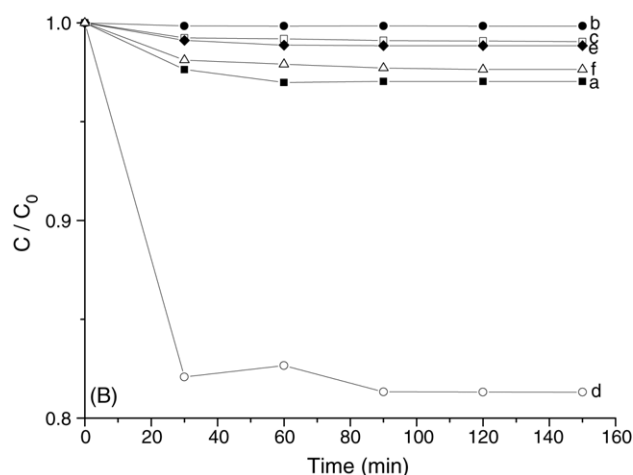


Fig. 4. Time course of the adsorption of MB (200 mL; $C_0 = 1.2 \times 10^{-5} \text{ mol L}^{-1}$) in the dark: (a) 24.5 mg TiO₂; (b) 0.5 mg sucrose-made carbon; (c) 0.5 mg commercial active carbon; (d) 25.0 mg CCT008, containing about 0.5 mg carbon; (e) mechanical mixture of 24.5 mg TiO₂ and 0.5 mg sucrose-made carbon; (f) slurry mixture of 24.5 mg TiO₂ and 0.5 mg active carbon.

titania treated at 600 °C has an anatase-type structure, but it is partly transformed to a rutile-type structure after calcined at 700 °C. On the other hand, CCT04-600 and CCT04-700 show similar XRD patterns, which are dominated by anatase phase. Obviously, the presence of carbon on the surface of titania inhibits its phase transformation, leading to a higher thermal stability.

3.2. Adsorption of methylene blue

Studies of adsorption of MB on powder samples were carried out in darkness. Fig. 4 shows the residual concentration of MB versus its original concentration as a function of adsorption time over various powder samples. The adsorption capacity of TiO₂-500 and sucrose carbon is both low, about 3.0% and 0.1%, respectively. Supposing that there is no interaction between carbon and titania, the adsorption capacity of CCT008-500 should be also low, as in the case of their slurry mixture [20–22]. However, 25.0 mg of CCT008-500 containing only 0.5 mg carbon shows an adsorption capacity of about 18.7%, much higher than any other samples. Since the specific surface area of CCT008-500 (98 m² g⁻¹) is similar to TiO₂-500 (100 m² g⁻¹), the increase in the adsorption capacity is not caused by the change of surface area. The unique adsorptive property of CCT should be related to its special surface property resulted from the uniform carbon deposition.

3.3. Photodegradation of methylene blue under UV illumination

Photodegradation of MB was tested over selected samples under UV illumination. The concentration of dye was monitored after 2 h magnetically stirring in darkness to secure

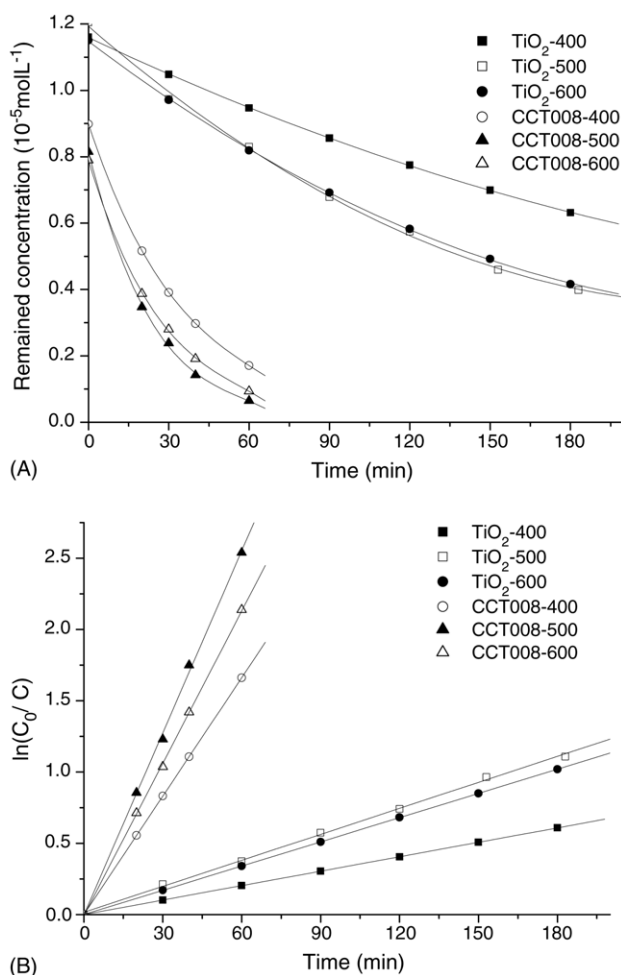


Fig. 5. (A) Curves of MB disappearance vs. reaction time in the presence of various catalysts under UV-illumination; (B) linear graph of $\ln(c_0/c)$ vs. time, transformed from (A).

the establishment of adsorption–desorption equilibrium before photocatalytic experiments. The curves of the photocatalytic disappearance of MB versus reaction time are shown in Fig. 5A. These curves are of the apparent first order as confirmed by the linear transforms of $\ln(c_0/c) \sim t$ as shown in Fig. 5B, from which the apparent rate constants can be obtained. The rate constant has been chosen as the basic kinetic parameter for the different systems, since it is independent of the concentration. As shown in Table 2, the CCT sam-

Table 2

Apparent rate constants k_{app} (10³ min⁻¹) of various UV or visible light illuminated solids

Sample	UV	Visible light
TiO ₂ -400	3.4	–
TiO ₂ -500	6.1	–
TiO ₂ -600	5.7	–
CCT008-400	28	6.9
CCT008-500	43	9.1
CCT008-600	36	6.7
P-25	30	–

ples exhibit much higher activity for MB photodegradation compared with the corresponding titania, even commercial Degussa P-25 TiO₂.

The surface modification of titania by carbon might be the critical reason for the improvement of the photocatalytic activity. Even if carbon can perturb the transmission of UV-light to the surface of titania, the increased adsorption capacity of CCT should benefit the photocatalytic degradation of the dyes. The carbon highly dispersed on the surface of titania adsorbs MB and then transfers it to the surface of titania. The driving force for this transfer is probably the difference in MB concentration between carbon and titania, as reported by Hermann and co-workers [20–22].

3.4. Photodegradation of methylene blue under visible-light illumination

The photodegradation activity of pure titania and CCT samples was also tested under visible light illumination in the same procedure. The curves of the photocatalytic disappearance of MB versus reaction time are presented in Fig. 6A. MB degrades by an apparent first-order kinetics in the presence of CCT powder as confirmed by the linear transforms of $\ln(c_0/c) \sim t$ as shown in Fig. 6B, while the concentration of MB decreases by an apparent zero-order kinetics on pure titania.

To understand the origin of the above phenomena, MB photobleaching was also conducted under visible light illumination without any photocatalysts, the results are shown in Fig. 6A. It can be found that the rate of MB photobleaching is almost the same as that of the decreasing of MB concentration over pure titania (TiO₂-400, TiO₂-500 and TiO₂-600), and the difference between the rate of the decrease of MB concentration over various pure titania under visible light illumination is not as obvious as that under UV illumination. In other words, pure titania does not show any activity under visible light illumination, viz., MB is only photobleached over pure titania. However, CCT samples show similar kinetic features as that under UV light illumination. Therefore, photodegradation of MB should be possible over CCT samples under visible light.

To confirm the mineralization of dyes over CCT samples under visible light, the concentration of the main products of MB degradation was measured. Generally, the anion of SO₄²⁻ is adopted to detect the photomineralization of dyes [34,35]. Table 3 shows the SO₄²⁻ concentration in the solution after photocatalytic reaction over TiO₂-500 and CCT008-500. A SO₄²⁻ concentration of 6.9 μmol L⁻¹ was detected in the solution containing CCT008-500 after 10 h of visible light illumination, which indicates that about 58% of sulphur from MB is converted to sulfate. But UV–vis spectroscopy shows that all the MB is converted, for no more MB can be detected. The lower conversion value deduced from SO₄²⁻ concentration might be resulted from the adsorption of sulfate. Lachheb et al. [35] also reported that sulfate produced by MB decomposition could be adsorbed

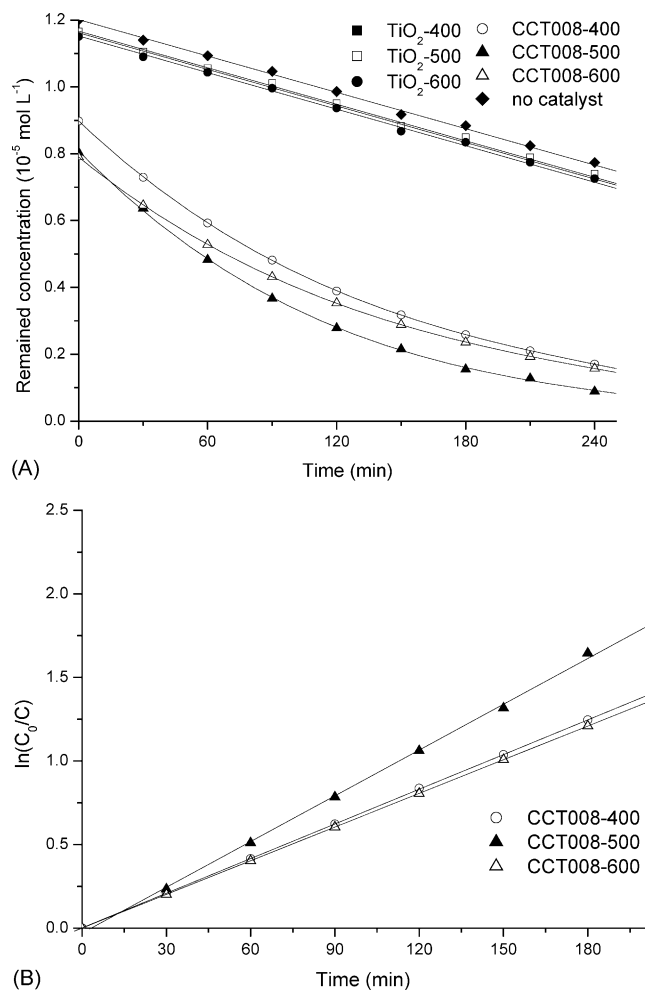


Fig. 6. (A) Curves of MB disappearance vs. reaction time in the presence of various catalysts under visible-light illumination; (B) linear graph of $\ln(C_0/C)$ vs. time for CCT008-400, CCT008-500 and CCT008-600, transformed from (A).

partially on the surface of the photocatalyst. Besides SO_4^{2-} , anions of NO_3^- and CO_3^{2-} with concentration about 16 and $82 \mu\text{mol L}^{-1}$, respectively, are also detected in the solution containing CCT008-500 after 10 h of visible light illumination. All these results suggest that MB has been mineralized largely rather than simply bleached at the present study. Oppositely, after the photocatalytic reaction over pure titania under visible light illumination, no SO_4^{2-} , NO_3^- or CO_3^{2-} was detected. It is proved again that MB has not been decomposed but only somewhat bleached over pure titania.

Table 3
 SO_4^{2-} , NO_3^- and CO_3^{2-} concentration in the solution containing TiO_2 -500 and CCT008-500 after 10 h of visible light illumination

	SO_4^{2-} ($\mu\text{mol L}^{-1}$)	NO_3^- ($\mu\text{mol L}^{-1}$)	CO_3^{2-} ($\mu\text{mol L}^{-1}$)
TiO_2 -500	0	0	0
CCT008-500	6.9	16	82

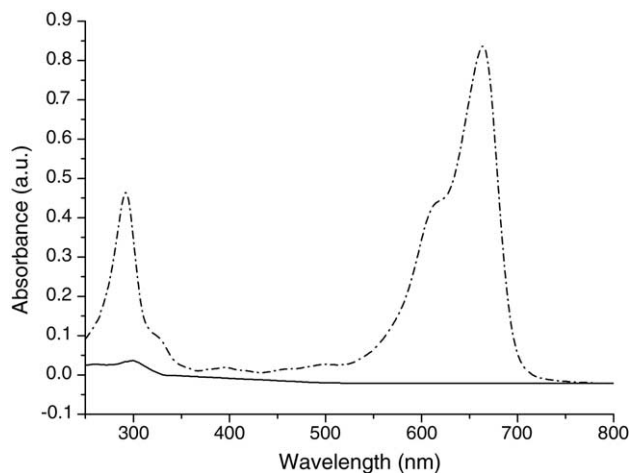


Fig. 7. The absorbance of MB solution before (dotted line) and after the photocatalytic reaction (solid line) under visible light for 10 h over CCT008-500.

Besides the observation of products of MB decomposition, the adsorption spectrum can also confirm the mineralization of MB over visible light illuminated CCT samples. Fig. 7 shows the absorbance of MB solution before and after photocatalytic reaction over CCT008-500. The peaks between 600 and 700 nm are assigned to the absorption of the conjugated π -system, while those peaks close to 300 nm are attributed to the absorption of aromatic ring [34,36]. It can be seen that all the original peaks disappear and no new peak can be observed after the photocatalytic reaction of 10 h, indicating that all aromatic rings in MB does not exist. This further proves that MB is decomposed rather than simply bleached over CCT samples under visible light irradiation. In other words, CCT samples are responsive to visible light, which may be attributed to the band-gap narrowing of titania.

UV–vis diffuse reflectance spectra can demonstrate the band-gap narrowing of titania in CCT above-mentioned. As shown in Fig. 8A, the new absorption of CCT008-500 above 400 nm is related to the containing carbon [5]. Assuming all the pure TiO_2 -500 and CCT008-500 to be indirect semiconductors, a plot of the modified Kubelka–Munk function versus the energy of exciting light [7] affords bandgap energies of 3.20 and 3.12 eV for TiO_2 -500 and CCT008-500, respectively (Fig. 8B). The band-gap narrowing of 0.08 eV is comparable with the value of 0.14 eV recently reported for carbon-modified titania with carbon content of 2.98% [7].

3.5. Long-time stability tests

In the long-time stability tests, 250 mg of selected catalyst CCT008-500 with the highest activity was irradiated under UV and visible-light, respectively, for 192 h. After every 24 h, aliquots of 25 mg of the used catalyst have been separated and subjected to standard reaction conditions for the determination of the remaining initial activity. Herein, the initial activity is defined as the conversion of MB after the first half

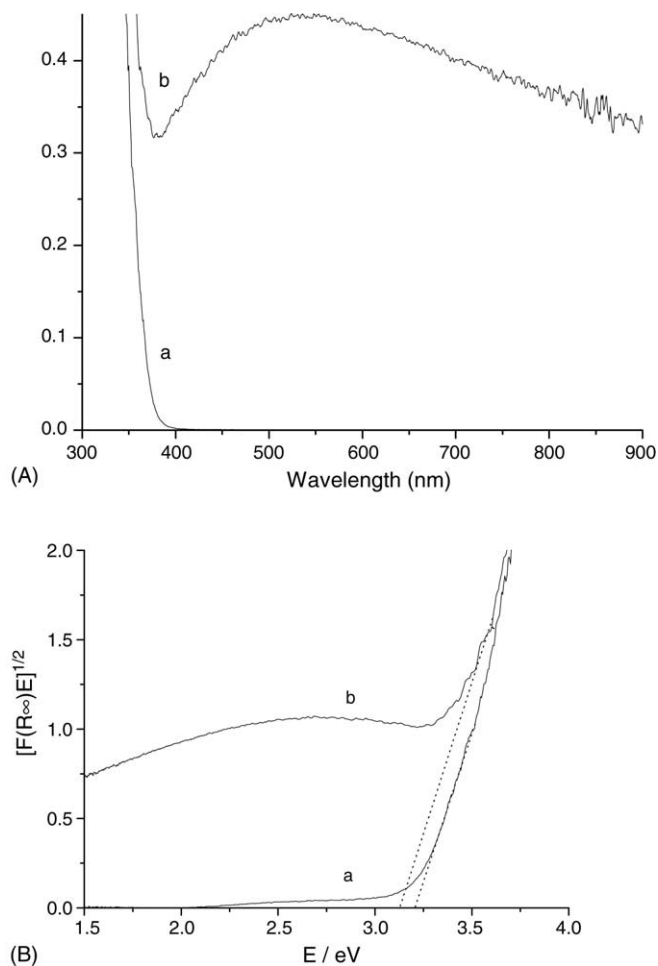


Fig. 8. (A) UV-vis diffuse reflectance spectra of TiO₂-500 (a) and CCT008-500 (b); (B) plot of transformed Kubelka–Munk function vs. the energy of the light absorbed.

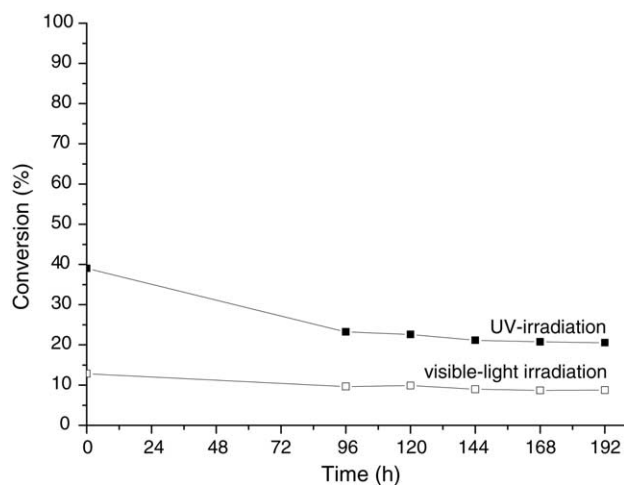


Fig. 9. Long-time stability tests of CCT008-500 under UV and visible-light irradiation.

hours photocatalytic reaction. As shown in Fig. 9, for the case of UV-irradiation, the initial activity of 39% conversion dropped to about 23% in this standard experiment after 96 h. From 96 to 192 h (24 h increments), no further activity loss can be observed and the stabilized activity (21–23% conversion) is still higher than the initial activity of TiO₂-500 (19% conversion). Similarly, under visible-light irradiation, after the decrease from 13% to 10%, the conversion is stabilized around 9%.

4. Conclusions

A novel and simple process has been developed for the synthesis of carbon-covered titania via pyrolysis of sucrose highly dispersed on the surface of titania in flowing N₂. Carbon covering the surface of titania can inhibit the TiO₂ phase transformation during calcinations, thus increases their thermal stability. For model pollutants, methylene blue, it is found that the adsorption capacity of CCT catalysts is much higher than that of the mixture of corresponding titania and carbon, which might be ascribed to its special surface property resulted from the uniform carbon deposition and the interaction with the dyes.

In addition, CCT catalysts show better photocatalytic properties than pure titania. Under UV illumination, the dyes' degradation in the suspension of CCT powders follows an apparent first-order kinetics, whose rate constant is much higher than pure titania, even commercial Degussa P-25 TiO₂. To be noted, carbon deposition makes the absorption edge of titania shift to the visible region. As a photocatalyst responsive to visible light, CCT shows kinetic features for the photodegradation of the dyes under visible light illumination similar to that under UV illumination. From the detection of the products of MB degradation, and the absorption spectra of MB solution after the photocatalytic reaction, it is proved that MB is decomposed rather than simply bleached over CCT samples under visible light illumination.

Acknowledgments

The authors are grateful to the National Science Foundation of China (20173002), and the Major State Basic Research Development Program (Grant no. G2000077503) for the financial support to this work.

References

- [1] O. Legrini, E. Oliveros, A. Braun, Chem. Rev. 93 (1993) 671.
- [2] W. Choi, A. Termin, M.R. Hoffmann, J. Phys. Chem. 98 (1994) 13669.
- [3] A. Fuerte, M.D. Hernandez-Alonso, A.J. Maira, A. Martínez-Arias, M.F. Gracia, J.C. Conesa, J. Soria, G. Munuera, J. Catal. 212 (2002) 1.
- [4] K.E. Karakitsou, X.E. Verkios, J. Phys. Chem. 97 (1993) 1184.

- [5] S.U.M. Khan, M. Al-Shahry, W.B. Ingler Jr., *Science* 297 (2002) 2243.
- [6] R. Asahi, T. Morikawa, T. Ohawaki, K. Aoki, Y. Taga, *Science* 293 (2001) 269.
- [7] S. Sakthivel, H. Kisch, *Angew. Chem. Int. Ed.* 42 (2003) 4908.
- [8] H. Irie, Y. Watanabe, K. Hashimoto, *Chem. Lett.* 32 (2003) 772.
- [9] T. Umabayashi, T. Yamaki, S. Tanaka, K. Assai, *Chem. Lett.* 32 (2003) 330.
- [10] T. Ohno, T. Mitsui, M. Matsumura, *Chem. Lett.* 32 (2003) 364.
- [11] J.C. Yu, J.G. Yu, W.K. Ho, Z.T. Jiang, L.Z. Zhang, *Chem. Mater.* 14 (2002) 3808.
- [12] T. Lindgren, J.M. Mwabora, E. Avendano, J. Jonsson, A. Hoel, C.-G. Granqvist, S.-E. Lindquist, *J. Phys. Chem. B* 107 (2003) 5709.
- [13] T. Ihara, M. Miyoshi, Y. Iriyama, O. Matsumoto, S. Sugihara, *Appl. Catal. B* 42 (2003) 403.
- [14] C. Lettmann, K. Hildenbrand, H. Kisch, W. Macyk, W.F. Maier, *Appl. Catal. B* 32 (2001) 215.
- [15] W. Zhao, W. Ma, C. Chen, J. Zhao, Z. Shuai, *J. Am. Chem. Soc.* 126 (2004) 4782.
- [16] H. Irie, S. Washizuka, N. Yoshino, K. Hashimoto, *Chem. Commun.* (2003) 1298.
- [17] H. Irie, Y. Watanabe, K. Hashimoto, *J. Phys. Chem. B* 107 (2003) 5483.
- [18] J.L. Gole, J.D. Stout, C. Burda, Y. Lou, X. Chen, *J. Phys. Chem. B* 108 (2004) 1230.
- [19] L. Lin, W. Lin, Y.X. Zhu, B.Y. Zhao, Y.C. Xie, *Chem. Lett.* 34 (2005) 284.
- [20] J. Matos, J. Laine, J.-M. Herrmann, *Appl. Catal. B* 18 (1998) 281.
- [21] J.-M. Herrmann, J. Matos, J. Disdier, C. Guillard, J. Laine, S. Malato, J. Blanco, *Catal. Today* 54 (1999) 255.
- [22] J. Matos, J. Laine, J.-M. Herrmann, *J. Catal.* 200 (2001) 10.
- [23] T. Tsumura, N. Kojitani, H. Umemura, M. Toyoda, M. Inagaki, *Appl. Surf. Sci.* 196 (2002) 429.
- [24] B. Tryba, A.W. Morawski, M. Inagaki, *Appl. Catal. B* 41 (2003) 427.
- [25] T. Tsumura, N. Kojitani, I. Izumi, N. Iwashita, M. Toyoda, M. Inagaki, *J. Mater. Chem.* 12 (2002) 1391.
- [26] M. Inagaki, Y. Hirose, T. Matsunaga, T. Tsumura, M. Toyoda, *Carbon* 41 (2003) 2619.
- [27] B. Tryba, T. Tsumura, M. Janus, A.W. Morawski, M. Inagaki, *Appl. Catal. B* 50 (2004) 177.
- [28] M. Janus, B. Tryba, M. Inagaki, A.W. Morawski, *Appl. Catal. B* 52 (2004) 61.
- [29] E. Carpio, P. Zuniga, S. Ponce, J. Solis, J. Rodriguer, W. Estrada, *J. Mol. Catal. A* 228 (2005) 293.
- [30] L. Lin, W. Lin, P. Wang, Y.X. Zhu, B.Y. Zhao, Y.C. Xie, *Acta Phys. Chim. Sin.* 10 (2004) 1179.
- [31] Y.C. Xie, Y.Q. Tang, *Adv. Catal.* 37 (1990) 1.
- [32] Y.X. Zhu, X.M. Pan, Y.C. Xie, *Acta Phys. Chim. Sin.* 15 (1999) 830.
- [33] M.S. Mel'gunov, V.B. Fenelonov, R. Leboda, B. Charnas, *Carbon* 39 (2001) 357.
- [34] J. Tang, Z. Zou, J. Yin, J. Ye, *Chem. Phys. Lett.* 382 (2003) 175.
- [35] H. Lachheb, E. Puzenat, A. Houas, M. Ksibi, E. Elaloui, C. Guillard, J.M. Hermann, *Appl. Catal. B* 39 (2002) 75.
- [36] P. Qu, J. Zhao, T. Shen, H. Hidaka, *J. Mol. Catal. A* 129 (1998) 257.